Chapter X

EPR on Flavoproteins

Richard Brosi*, Robert Bittl, Christopher Engelhard*

Summary

Flavoproteins often employ radical mechanisms in their enzymatical reactions. This involves paramagnetic species, which can ideally be investigated with EPR spectroscopy. In this chapter, we focus on the example of flavin based photoreceptors and discuss, how different EPR methods have been used to extract information about the flavin radical's electronic state, its binding pocket environment, electron transfer pathways, and about the protein's tertiary and quaternary structure.

Keywords: ENDOR spectroscopy, radical mechanisms, photoreceptors, transient EPR, protein structure

1. Introduction

The function of flavoproteins is often based on the radical mechanisms of electron or hydrogen atom transfer reactions resulting in the change of the oxidation (and protonation) state of the flavin (Fl) cofactor [1-8]. Flavins can exist in three redox states – the fully oxidized, the one-electron reduced semiquinone (radical), and the fully reduced hydroquinone forms [9]. The semi- and the hydroquinone forms exist in two different physiologically relevant protonation states, respectively. Electron Paramagnetic Resonance (EPR) methods are ideally suited to investigate the Fl semiquinone radical forms of flavoproteins if a) the catalytic cycle natively involves radical species or b) those in which radicals can be induced artificially, e.g. after mutagenesis.

The key advantage of EPR methods is the intrinsic simplification of the observed system to the radical molecule and only those parts of a protein that interact with it. As a non- or minimally invasive method, EPR allows for the investigation of these systems in a functional state [10-12] or even under *in cell* conditions [13].

The EPR signal of the Fl semiquinone at X-band is characterized by one resonance line of almost gaussian shape. It has a width of about 3mT

Full-Width Half-Maximum (FWHM), which is a typical width for an organic radical and is small in comparison to paramagnetic metal centers. Its spin-lattice relaxation is very slow (up to 2s at 5K) and accordingly cw spectra have to be acquired with very low microwave power to avoid saturation, while pulse spectra require very low repetition rates. By using higher magnetic fields, the homogenous X-band spectrum can be resolved into the three fundamental *g*-components, each additionally split by the hyperfine interaction. For an extensive discussion of the cw EPR spectrum and its saturation behavior, see Chapter 7, Vol. 131 of the first edition of this series [14].

In this chapter we will focus on questions that can be addressed by advanced EPR spectroscopic methods and illustrate how the different interactions that involve the Fl semiquinone radical can be exploited in order to obtain specific information. Thereby, we discuss intra-flavin effects, interactions between the flavin and its direct protein environment and long range couplings between the Fl radical and other radicals.

2. Characterization of the Electronic Structure of Flavin Radicals

The most fundamental question that arises in studies of flavoproteins is the characterization of the Fl oxidation state during protein function. In general, the different Fl oxidation states can be readily discerned by their UV/Vis absorption and emission properties which yield characteristic colors of flavoprotein solutions [15,16]. However, often it is difficult to conclude on the *in vivo* Fl oxidation states from *in vitro* studies of isolated protein solutions. This identification of the Fl oxidation state is of particular interest in flavoproteins with function other than electron shuttling between redox active partner proteins. Here, EPR can help to distinguish between different functional states of the protein. As an example, the dark state of the blue-light photoreceptor cryptochome (Cry) was shown to contain a diamagnetic Fl species by the absence of any EPR signal under *in cell* conditions. On the other hand, an EPR signal grows in a cell suspension expressing Cry upon blue-light illumination. Such a signal is absent in control cells not expressing Cry. Thus, the blue-light induced signaling state of Cry can be associated with the paramagnetic state of the flavoprotein, i.e. contains the Fl semiquinone form. In conjunction with the formation of the semiquinone state upon light excitation, the dark state can be associated with the fully oxidized Fl.

When a Fl semiquinone radical is established as a functional intermediate in the protein function, the question about its protonation state arises: Is it either the anionic radical ($Fl^{\bullet -}$) generated by electron transfer, or the neutral radical ($FlH^{\bullet}$) protonated at N(5) (figure 1, bottom) created by subsequent protonation of $Fl^{\bullet -}$ or direct hydrogen atom transfer to a Fl. Two characteristic magnetic interactions distinguish between both species, a) the *g*-matrix [13,17,18] representing the anisotropic coupling of the spin magnetic moment to an external magnetic field, and b) the hyperfine couplings of nuclei carrying a magnetic moment with the

unpaired electron spin. In Fl, the isoalloxazine protons and H1' (see figure 1 for the IUPAC naming convention) show significant coupling to the electron spin [19–27]. The main electronic effect observed is a rearrangement of spin density from N(5) and N(10) into the xylene ring upon deprotonation of N(5) [28,29].

In EPR spectroscopy the differences in the *g*-matrix become observable under high-field conditions (for Fl, microwave frequencies at about 100 GHz and above) where a fingerprint *g*-matrix for the respective species could be established (figure 1) [20,30,31].

[Figure 1 360 GHz spectra of neutral and anionic radical]

Hyperfine couplings can be detected precisely and with high resolution utilizing the EPR based Electron Nuclear DOuble Resonance (ENDOR) spectroscopy. There, two resonance lines arise for each nucleus experiencing hyperfine coupling with a coupling constant *A* to the unpaired electron spin. Several excellent reviews exist explaining in detail both the basics of ENDOR and its applications to biomolecules [34-36].

In flavins, several proton couplings are detectable by ENDOR (see figure 2). These couplings derive from the protons attached to C(6), C(7α), C(8α), C(9), C(1') and N(5). The couplings of H(7α) and H(9) are very small and are better visible by selectively deuterating these positions. The coupling originating from H(5) is especially useful, because the protonation state of the Fl semiquinone state is directly visible in the presence or absence of ENDOR signal stemming from the present or absent proton at N(5) in the neutral ($FlH^{\bullet}$) or the anionic ($Fl^{\bullet -}$) species, respectively. Additionally, a significant rearrangement of spin density within the isoalloxazine moiety is found between the two semiquinone protonation states. This leads to changes in the hyperfine coupling constants apparent in the ENDOR spectrum of $Fl^{\bullet}$ (figure 3) as a substantial increase of the hyperfine splittings of H(8α) and H(6) as well as a decrease of the H(1') coupling in the neutral radical state [20].

[Figure 2 Different hyperfine couplings detected with different methods]

[Figure 3 ENDOR of glucose oxidase at different pH values]

Thus, EPR and ENDOR offer excellent methods for the identification of the Fl redox and protonation states not only in protein solution but also in whole cells [13], where UV/Vis spectroscopy often fails.

3. Characterization of the Local Surrounding of a Flavin Radical

The spin density distribution within a radical is sensitive not only to substantial changes at the radical itself, e.g. changes of the protonation state as discussed above, but to subtle changes in the radical's environment. Therefore, hyperfine spectroscopy can be used as a local probe for the protein surrounding of a Fl radical.

This principle, e.g., has been successfully employed in the investigation of the photocycle of *Xenopus laevis* (6-4) photolyase [22]. (6-4) photolyases are repair enzymes which can restore the UV-generated pyrimidine(6-4)pyrimidone DNA lesion [5,6] by a light-activated two-step repair cycle after binding to the damaged DNA [37–39]. A detailed reaction scheme has been proposed [40], based on a comparison to the well understood CPD photolyases that repair a different type of UV damage, the cyclobutane pyrimidine dimer, via a catalytic radical reaction cycle [41]. A noteworthy difference in their mechanisms is the pronounced dependence of (6-4) photolyase activity on the pH value [42,43]. In the proposed reaction scheme, two highly conserved histidines (His354, His358 in *X. laevis* (6-4) photolyase) are essential to the reaction, with one of them acting as proton donor and the other as proton acceptor.

An ENDOR study focused on assigning which histidine plays which role as well as investigating their location with respect to the flavin [22]. To achieve this, two mutations of *X. laevis* (6-4) photolyase, His354Ala and His358Ala, were examined at two pH values and compared to the wild type (WT). While incapable of photo-repair, they still undergo activation by photoreduction. The ENDOR spectra of both the WT and the mutation lacking His354 (His354Ala) showed distinct differences between pH 6 and pH 9.5, while His358Ala showed no such dependence (figure 4). Therefore, histidine 354 retains its protonation state irrespective of two examined external pH values. At pH 9.5, the H1' hyperfine coupling is considerably diminished in His354Ala compared to the WT and to His358Ala, which can be conceived as the effect of a rearrangement of the ribityl side chain upon replacement of His354 with a smaller alanine, thus demonstrating His354's proximity to the ribityl side chain [22].

Strong changes in the H(1') hyperfine coupling as well as a change of the intensity of the H(8α) signal are observed when comparing the spectra of His354Ala at pH 6 and pH 9.5. This implies a conformational change of His358 caused by protonation/deprotonation. While the changes in the H(1') hyperfine coupling are absent in the WT, it exhibits an identical change in signal intensity of H(8α), proving that the same protonation change also happens in the wild type (The lack of change in H(1') is most likely due to mutual stabilization of both histidines). His354 retains its protonation regardless of pH, while His358 loses its proton in alkaline condition at pH 9.5. As the proposed reaction mechanism requires an initially protonated histidine and it is functional at pH 6 as well as at

pH 9.5, consequently only His354 can act as proton donor, while His358 is the proton accepting reaction partner.

[Figure 4: *X. laevis* 6-4 PL ENDOR –\ 2 Histidines]

A second example for the use of hyperfine spectroscopy to locally probe the protein environment of a Fl radical involves the blue-light active LOV domains. They are widely present in plant, fungal and bacterial proteins [44,45] and are distinguished from other flavin-based photoreceptors by the formation of a covalent bond between the flavin cofactor at the C(4a) position and a conserved nearby cysteine residue. The so-called C(4a)-cysteinyl adduct arising upon blue-light illumination [46-48] marks the initial step in the creation of the protein's active state, thus the adduct lifetime is closely associated with the biological function. In spite of their similar amino acid sequence and 3D structure [49-51], individual LOV domains vary strongly in this parameter, with dark recovery ranging from seconds in some plant phototropins up to virtually irreversible photoreactions in some bacterial LOV proteins [52,53]. It is therefore reasonable to assume that only small structural deviations in the flavin binding pocket induce these substantial differences. As we have discussed earlier, small conformational changes in the vicinity of a flavin radical are readily observable by ENDOR spectroscopy. The question then arises whether such changes can be related to changes in the duration of the protein's photocycle.

To this end, an ENDOR study on the LOV2 domain of *Avena sativa* (*A. sativa*) photoropin 1 was performed. In order to render the system accessible to EPR methods, formation of the C(4a) photoadduct was inhibited by replacing the cysteine with an alanine. Thereby, instead of adduct formation the photoexcited flavin becomes reduced and converts to the neutral radical state [21].

The three protons of a methyl group coupled to an unpaired electron spin usually give rise to only one unresolved line in ENDOR. This is due to a rotation of the methyl group that is typically fast on the time scale of the experiment even down to very low temperatures (less than 10K). [20-22]. However, the ENDOR spectrum of the inhibited (non-C(4a) adduct-producing) LOV2 domain (Cys450Ala) shows a three component splitting of the averaged H(8α) line even at temperatures as high as 110 K, indicating that the methyl group rotation is hindered within the *A. sativa* phototropin 1 LOV2 domain binding pocket.

To determine which amino acids cause this effect, ENDOR measurements of various mutations in the vicinity of the 8α group were performed. Large variations in the H(8α) couplings as well as widely differing temperature dependencies of the methyl group mobility were discovered (figure 5). Simulation of the spectra in addition to DFT calculations allows the determination of the frozen i.e. immobilized sidegroup's angle with respect to the isoalloxazine plane [21].

One mutation in particular, Asn425Cys, possesses a substantially different angle as well as a much lower freezing temperature (figure 6). This mutation was designed with homology to another LOV domain in mind, *Chlamydomonas reinhardtii* (*C. reinhardtii*) phototropin 1 LOV2, and comparison of their respective ENDOR spectra and temperature dependence showed a striking similarity. Additionally, the Asn425Cys mutant's photoadduct lifetime was drastically reduced compared to the wild type, thus bringing it much closer to the adduct lifetime of *C. reihardtii* [21] (Dark recovery time constants: *A. sativa* WT – 50.3 s, *A. sativa* Asn425Cys – 7.6 s, *C. reinhardtii* WT – 20 s [54].).

[Figure 5: ENDOR of As LOV2 mutants]

[Figure 6: DFT of 8α rotation, Comparison N425C to *C. reinhardtii* LOV2]

Hence Asn425 appears to stabilize the conformation of the isoalloxazine moiety of the flavin, thus strengthening the intrinsically weak C(4a)–S-bond and thereby increasing the lifetime of the photoadduct. Replacing this asparagine with another amino acid (for example, a cysteine in homology to *C. reinhardtii*) restores some conformational flexibility to the flavin, with an accompanying reduction in photoadduct lifetime.

In LOV domains, the covalent bond is formed between a cysteine residue and the flavin cofactor. Adduct formation between the flavin and other residues is possible as well. In a cognate LOV1 domain from *C. reinhardtii*, it was shown with ENDOR and high field EPR spectroscopy that the bond formation can also take place between the flavin and an artificially introduced methionine residue [55]. This mutant offers unique insights into the process of adduct formation. Generally, it was thought that transfer of a proton initialized the bond formation, but here using the sensitivity to proton couplings, it was possible to show that protonation does not occur in the C57M mutant. Instead a transient radical pair is created before adduct formation and subsequent oxidation of the flavin into the neutral radical form. The proposed full photoreaction scheme comprises a complete pathway for the mechanism of C(4a) adduct formation, suggesting that wildtype adduct formation starts with a radical pair as well and not – as had been previously proposed – with the protonation of the flavin.

So far we have focused on ENDOR as the mainly used hyperfine spectroscopy technique. While ENDOR spectroscopy is a very sensitive tool for investigating hyperfine couplings larger than about 1 MHz, more weakly coupled nuclei or those with small Larmor frequencies are often difficult to observe by this technique. In the case of flavins, many of the protons of the isoalloxazine moiety have hyperfine couplings sufficient for detection by ENDOR (see above), however some contain couplings which are difficult to detect. Furthermore, the nitrogen nuclei in the pyrazine and pyrimidine rings of the Fl escape direct observation at standard EPR/ENDOR frequencies of 9 GHz (X-Band).

This information gap can be filled by time domain electron spin echo techniques. The Electron Spin Echo Envelope Modulation (ESEEM) effect enables detection of hyperfine couplings as modulation frequencies in a spin echo experiment with variable pulse separation times. 1D, 2D ESEEM, and HYperfine Sublevel CORrElation (HYSCORE) spectroscopy were successfully applied in a study on neutral and anionic flavin radicals in Flavodoxin, where for the first time distinct couplings of the electron spin to the nitrogen atoms in the isoalloxazine moiety could be determined [56,57]. The electronic structure of the isoalloxazine ring was shown to be sensitive to the aromatic amino acids Trp57 and Tyr94 close to the Fl cofactor in a mutational study on Flavodoxin from *Anabaena* PCC 7119 [57] .

As discussed so far, a flavin radical is a highly sensitive probe for the immediate protein surrounding of the isoalloxazine moiety [22]. Additionally, it is even feasible to detect and interpret influences from remote molecules and the polarity of the flavin binding pocket. *Escherichia coli* CPD photolyase was subject of a study [58] to investigate the binding of the DNA CPD lesion to the protein [40], which is the prerequisite for the repair reaction. This was achieved by comparing pure photolyase protein solution with a sample containing UV irradiated oligo$(dT)_{18}$ DNA substrate bound to the protein in the dark. Binding of the substrate within a short distance to the flavin would lead to additional hyperfine couplings from substrate protons to the unpaired electron spin. Such couplings would be expected in the so-called matrix region of the ENDOR spectrum that is within 1.25 MHz of the central proton frequency [59, 60].

When comparing the ENDOR spectra of both samples, only very slight differences including a drop in intensity in the matrix region were noticeable (figure 7). These changes, however, are far too small to be interpreted as the kind of steric alterations in the binding pocket discussed above [21]. Since no additional features appeared in the matrix region, it was concluded that the substrate does not come within 0.6 nm to the flavin [60], a finding corroborated later by an X-ray crystallographic study [61].

[Figure 7: cw ENDOR of *E. coli* CPD PL –\ Substrate binding]

The observable drop in intensity in the matrix region could be caused by water molecules being removed from the binding pocket, thus reducing its overall polarity. DFT calculations show that this alteration in polarity should also affect the hyperfine couplings [58]. Indeed, such changes were observed in the H(1'), H(6) and H(8α) signals, with those for H(6) smaller than for the other protons, indicating that H(6) is less exposed. This again was later confirmed by the crystal structure [61].

Hyperfine spectroscopy in the form of ENDOR or ESEEM methods on flavins and other semiquinones is thus shown to be a precise and highly sensitive method to investigate subtle changes in the radical's

environment. However, in special cases Fl radicals can also be reporter molecules for long-range properties, e.g. measurements of intra- or even inter-protein distances.

4. Long-range interactions

4.1 Transient EPR in the investigation of radical pairs

To examine fast reactions like electron transfer involving radical pairs or short lived spin polarized triplet states in the time domain, transient EPR is employed [62,63]. It is usually implemented as a cw EPR technique where a laser flash triggers the light-dependent formation of the spin system. By avoiding the lock-in detection of standard cw-EPR, the time resolution for acquisition of the radical species' evolution can be pushed into the few nanosecond range [64-66].

Interesting examples of short-lived radical pairs occur in DNA photolyases and Cry proteins upon illumination with blue light. These two protein classes show high homology, in sequence as well as in structure [6, 67]. Both Cry and photolyases can undergo a light-induced process, the so-called "light activation", whereupon the fully oxidized flavin abstracts an electron from either a nearby tryptophan or tyrosine residue leading to the formation of a radical pair [68, 69]. While the DNA repair mechanism discussed above is uncommon in Cry [5,6], they were shown to be essential mediators of the circadian clock [70-72] as well as light sensors for plant sprouting [73,74].

Point mutation studies in *E. coli* CPD photolyase that replaced each individual tryptophan showed that only the W306F mutant prevented photoreduction [75], proving that Trp306 is the terminus of the electron transfer chain. As the distance between the flavin isoalloxazine moiety and Trp306 is too large for a fast direct electron transfer on the order of 30 ps [76], the electron transfer has to be mediated through a chain of electron donors. In *E. coli* CPD photolyase two tryptophans, TRp359 and Trp382, connect the isoalloxazine moiety of FAD with Trp306 [40]. This amino-acid chain is completely conserved throughout all structurally characterized photolyases and is also found in cryptochromes. These tryptophans have early on been postulated to be the main electron transfer pathway [77]. For *Arabidopsis* Cry1 it has been demonstrated that substitution of the chain's first and third tryptophan impairs both light induced electron transfer in vitro as well as the photoreceptor function *in vivo* [78], demonstrating the biological relevance of this mechanism.

Transient EPR was applied to detect the short lived radical pair formed by the flavin and the terminal tryptophan [10]. The shape of this radical pair signal drastically depends on the initial spin state before separation of the two electrons. If the initial state is a pure singlet, the number of spins with spin up and spin down projections are equal, i.e. the net spin polarization is zero. Therefore the integrated trEPR signal amplitude over

the field range also amounts to zero, i.e. emissive and absorptive components cancel.

If in contrast to that the initial state has (a least partial) triplet character, a net spin polarization is expected depending on the different occupation of the high and low energy triplet state sublevels T_+ and T_- in an external magnetic field. Specifically, if the radical pair is formed rapidly while the system remains in a spin state with strong T_+ or T_- character, a net polarization that decreases with higher magnetic field is expected. If however, the initial state's spin relaxation is fast enough for thermalization, the net polarization is expected to increase with higher magnetic field. For a detailed explanation of this effect, see [10,11]. In case of *Xenopus laevis* cryptochrome-DASH, spectra measured at both X- and Q-band frequencies show no net absorption or emission, whereas simulations of a thermalized and fully polarized triplet precursor predict a net absorptive spectrum at Q-band or a net emissive spectrum at X-band, respectively, thus leaving the singlet precursor as the only possible origin state of the precursor (figure 8) [10].

[Figure 8: Xcry + different precursors]

Even though the Trp chain is conserved throughout photolyases and cryptochromes, the electron transfer does not necessarily have to follow this route. Mutation studies on *Synechocystis* Cry-DASH have shown that in this cryptochrome the distal tryptophan Trp320 (structurally equivalent to Trp306 in DNA photolyase) is not the terminal electron donor [12] (figure 9). Instead of a transfer via Trp396-Trp373-Trp320, as expected from *Xenopus laevis* Cry-DASH, the actual transfer chain is Trp396-Trp373-Trp375. Even though the distance from Trp375 to Trp373 is 8.2 Å compared to 3.7 Å between Trp320 and Trp373, their aromatic ring systems are more suitably oriented to transfer the electron. Furthermore, Trp375 is likely more accessible to solvent molecules and thus more easily stabilized by deprotonation and solvent-radical interaction.

[Figure 9: XCry structure + SCry structure + trEPR spectra]

Obviously, subtle differences between species can have dramatic effects on the protein function that are not readily deducible from the amino acid sequence or even the crystal structure alone. Here transient EPR was shown to be a valuable tool to investigate these dynamic processes.

4.2 ELDOR spectroscopy

(Pulsed) Electron-Electron DOuble Resonance ((p)ELDOR, also known as Double Electron-Electron Resonance (DEER)) [79,80] has emerged as

an immensely popular tool for the measurement of inter-spin distances [81]. When it is applied to conformational analysis of proteins, ELDOR usually involves attaching spin labels at predetermined positions using site directed-spin labeling [82,83]. The disadvantage of this procedure is, besides the effort necessary to produce mutants with labeling sites not influencing the structure or function of the protein, that the rather flexible spin labels often result in broad and therefore hard to analyze distance distributions [84].

One possibility to reduce this problem is to generate a radical state in a protein natively containing a flavin or another redox-active chromophore. Recently, it has been shown that the FAD bound to the *Parococcus denitrificans* ETF protein can be used in such a way [85] when enzymatically reduced to its anionic radical form. In this study, the authors could detect two separate conformations of the protein by analyzing the distances between the flavin radical and one additional spin label.

An earlier study centered on the determination of the flavin-flavin distance in augmenter of liver regeneration (ALR) dimers [86]. There, the authors could establish a 2.6 nm distance between the neutral flavin radicals within the dimer. The rather localized spin density distribution in $Fl^{\bullet}$ around C(4a) and N(5) carries a high potential for this ELDOR-based approach to enable the study of dimerization/multimerization states and conformational changes in flavoproteins.

5. Conclusion

We have shown that EPR techniques have very broad applications in the study of flavins and flavoproteins:

- EPR on a single electron spin will only detect interactions centered around this spin probe, thus it is selective to the very localized surrounding and can precisely detect subtle effects and changes.
- At the same time, large distance interactions between several electron spins can be detected with EPR methods as well. This provides access to investigation of larger conformational changes and radical pairs.
- Finally, transient EPR has emerged as a tool to analyze time dependent dynamics in electron transfer processes.
- As an additional boon, many EPR experiments can be performed at or close to physiological conditions or even *in vivo* [13].

Modern EPR techniques will certainly continue to play a pivotal role in the investigation of the function of biological systems.

6. Acknowledgements

We thank the UniCat Cluster of Excellence for funding.

References

[1] Frey PA, Hegemann AD, Reed GH (2006) Free radical mechanisms in enzymology. *Chem Rev* **106**, 3302-3316

[2] Losi A (2007) Flavin-based blue-light photosensors: A photobiophysics update. *Photochem Photobiol* **83**, 1283-1300

[3] Demarsy E, Fankhauser C (2009) Higher plants use LOV to perceive blue light. *Curr Opin Plant Biol* **12**, 69-74

[4] Losi A, Gärtner W (2011) Old Chromophores, New Photoactivation Paradigms, Trendy Applications: Flavins in Blue Light-Sensing Photoreceptors. *Photochem Photobiol* **87**, 491-510

[5] Weber S (2005) Light-driven enzymatic catalysis of DNA repair: a review of recent biophysical studies on photolyase. *Biochim Biophys Acta* **1707**, 1-23

[6] Sancar A (2003) Structure and function of DNA photolyase and cryptochrome blue-light photoreceptors. *Chem Rev* **103**, 2203-2237

[7] Müller M, Carell T (2009) Structural biology of DNA photolyases and cryptochromes. *Curr Opin Struct Biol* **19**, 277-285

[8] Massey V (1994) Activation of molecular oxygen by flavins and flavoproteins. *J Biol Chem* **269**, 22459-22462

[9] Massey V, Palmer G (1966) On the existence of spectrally distinct classes of flavoprotein semiquinones. A new method for quantitative production of flavoprotein semiquinones. *Biochemistry* **5**, 3181

[10] Weber S, Biskup T, Okafuji A, Marino AR, Berthold T, Link G, Hitomi K, Getzoff ED, Schleicher E, Norris JR (2010) Origin of Light-Induced Spin-Correlated Radical Pairs in Cryptochrome. *J Phys Chem B* **114**, 14745-14754

[11] Mi QX, Ratner MA, Wasielewski MR (2010) Time-Resolved EPR Spectra of Spin-Correlated Radical Pairs: Spectral and Kinetic Modulation Resulting from Electron-Nuclear Hyperfine Interactions. *J Phys Chem A* **114**, 162-171

[12] Biskup T, Hitomi K, Getzoff ED, Krapf S, Koslowski T, Schleicher E, Weber S (2011) Unexpected Electron Transfer in Cryptochrome Identified by Time-Resolved EPR Spectroscopy. *Angew Chem Int Ed* **50**, 12647-12651

[13] Schleicher E, Wenzel R, Ahmad M, Batschauer A, Essen LO, Hitomi K, Getzoff ED, Bittl R, Weber S, Okafuji A (2010) The Electronic State of Flavoproteins: Investigations with Proton Electron-Nuclear Double Resonance. *Appl Magn Res* **37**, 339-352

[14] Murataliev, MB (1999) Applications of Electron Spin Resonance (ESR) for Detection and Characterization of Flavonprotein Semiquinones. Methods Mol Biol **131**, 97-110

[15] Müller F (1981) Spectroscopy and photochemistry of flavins and flavoproteins. *Photochem Photobiol* **34**, 753-758

[16] Heelis PF (1982) The photophysical and photochemical properties of flavins (isoalloxazines). *Chem Soc Rev* **11**, 15-39

[17] Weber S, Kay CWM, Bacher A, Richter G, Bittl R (2005) Probing the N(5)-H bond of the isoalloxazine moiety of flavin radicals by X- and W-band pulsed electron-nuclear double resonance. *Chemphyschem* **6**, 292-299

[18] Acocella A, jones GA, Zerbetto F (2010) What Is Adenine Doing in Photolyase? *J Phys Chem B* **114**, 4101-4106

[19] Barquera B, Morgan JE, Lukoyanov D, Scholes CP, Gennis RB, Nilges MJ (2003) X- and W-band EPR and Q-band ENDOR studies of the flavin radical in the Na+-translocating NADH : quinone oxidoreductase from Vibrio cholerae. *J Am Chem Soc* **125**, 265-275

[20] Okafuji A, Schnegg A, Schleicher E, Möbius K, Weber S (2008) G-tensors of the flavin adenine dinucleotide radicals in glucose oxidase: A comparative multifrequency electron paramagnetic resonance and electron-nuclear double resonance study. *J Phys Chem B* **112**, 3568-2574

[21] Brosi R, Illarionov B, Mathes T, Fischer M, Joshi M, Bacher A, Hegemann P, Bittl R, Weber S, Schleicher E (2010) Hindered Rotation of a Cofactor Methyl Group as a Probe for Protein-Cofactor Interaction. *J Am Chem Soc* **132**, 8935-8944

[22] Schleicher E, Hitomi K, Kay CWM, Getzoff ED, Todo T, Weber S (2007) Electron nuclear double resonance differentiates complementary roles for active site histidines in (6-4) photolyase. *J Biol Chem* **282**, 4738-4747

[23] Kurreck H, Bock M, Bretz N, Elsner M, Kraus H, Lubitz W, Müller F, Geissler J, Kroneck PMH (1984) Fluid solutions and solic-state electron nuclear double resonance studies of flavin model compounds and flavoenzymes. *J Am Chem Soc* **106**, 737-746

[24] Cinkaya I, Buckel W, Medina M, Gomez-Moreno C, Cammack R (1997) Electron-nuclear double resonance spectroscopy investigation of 4-hydroxybutyryl-CoA dehydratase from Clostridium aminobutyricum: Comparison with other flavin radical enzymes. *Biol Chem* **378**, 843-849

[25] Medina M, Lostao A, Sancho J, Gomez-Moreno C, Cammack R, Alonso PJ, Martinez JI (1999) Electron-nuclear double resonance and hyperfine sublevel correlation spectroscopic studies of flavodoxin mutants from Anabaena sp PCC 7119. *Biophys J* **77**, 1712-1720

[26] Kay CWM, Feicht R, Schulz K, Sadewater P, Sancar A, Bacher A, Mobius K, Richter G, Weber S (1999) EPR, ENDOR, and TRIPLE resonance spectroscopy on the neutral flavin radical in Escherichia coli DNA photolyase. *Biochemistry* **38**, 16740-16748

[27] Kay CWM, El Mkami H, Molla G, Pollegioni L, Ramsay RR (2007) Characterization of the covalently bound anionic flavin radical in monoamine oxidase a by electron paramagnetic resonance. *J Am Chem Soc* **129**, 16091-16097

[28] Weber S, Möbius K, Richter G, Kay CWM (2001) The electronic structure of the flavin cofactor in DNA photolyase. *J Am Chem Soc* **123**, 3790-3798

[29] Garcia JI, Medina M, Sancho J, Alonso PJ, Gomez-Moreno C, Mayoral JA, Martinez JI (2002) Theoretical analysis of the electron spin density distribution of the flavin semiquinone isoalloxazine ring within model protein environments. *J Phys Chem B* **106**, 4729-4735

[30] Fuchs MR, Schleicher E, Schnegg A, Kay CWM, Törring JT, Bittl R, Bacher A, Richter G, Mobius K, Weber S (2002) g-tensor of the neutral flavin radical cofactor of DNA photolyase revealed by 360-GHz electron paramagnetic resonance spectroscopy. *J Phys Chem B* **106**, 8885-8890

[31] Schnegg A, Okafuji A, Bacher A, Bittl R, Fischer M, Fuchs MR, Hegemann P, Joshi M, Kay CWM, Richter G, Schleicher E, Weber S (2007) Towards an identification of chemically different flavin radicals by means of their g-tensor. *Appl Magn Res* **30**, 345-358

[32] Kay CWM, Schleicher E, Hitomi K, Todo T, Bittl R, Weber S (2005) Determination of the g-matrix orientation in flavin radicals by high-rield/high-frequency electronnuclear double resonance. *Magn Reson Chem* **43**, S96-S102

[33] Kay CWM, Bittl R, Bacher A, Richter G, Weber S(2005) Unambiguous determination of the g-matrix orientation in a neutral flavin radical by pulsed electron-nuclear double resonance at 94 GHz. *J Am Chem Soc* **127** 10780-10781

[34] Murphy DM, Farley RD (2006) Principles and applications of ENDOR spectroscopy for structure determination in solution and disordered matrices. *Chem Soc Rev* **35**, 249-268

[35] Van Doorslaer S, Vinck E (2007) The strength of EPR and ENDOR techniques in revealing structure-function relationships in metalloprotein. *Phys Chem Chem Phys* **9**, 4620-4638

[36] Kulik L, Lubitz W (2009) Electron-nuclear double resonance. *Photosynth Res* **102**, 391-401

[37] Kim ST, Malhotra K, Smith CA, Taylor JS, Sancar A (1994) Characterization of (6-4)-photoproduct DNA photolyase. *J Biol Chem* **269**, 8535-8540

[38] Zhao XD, Liu JQ, Hsu DS, Zhao SY, Taylor JS, Sancar A (1997) Reaction mechanism of (6-4) photolyase. *J Biol Chem* **272**, 32580-32590

[39] Hitomi K, Kim ST, Iwai S, Harima N, Otoshi E, Ikenaga M, Todo T (1997) Binding and catalytic properties of Xenopus (6-4) photolyase. *J Biol Chem* **272**, 32591-32598

[40] Park HW, Kim ST, Sancar A, Deisenhofer J (1995) Crystal-structure of DNA photolyase from Escherichia coli. *Science* **268**, 1866-1872

[41] Jordan SP, Jorns MS (1988) Evidence for a singlet intermediate in catalysis by Escherichia coli DNA photolyase and evaluation of substrate binding determinants. *Biochemistry* **27**, 8915-8923

[42] Hitomi K, Nakamura H, Kim ST, Mizukoshi T, Ishikawa T, Iwai S, Todo T (2001) Role of two histidines in the (6-4) photolyase reaction. *J Biol Chem* **276**, 10103-10109

[43] Lv XY, Qiao DR, Xiong Y, Xu H, You FF, Cao Y, He X, Cao Y (2008) Photoreactivation of (6-4) photolyase in Dunaliella salina. *FEMS Microbiol Lett* **283**, 42-46

[44] Christie JM (2007) Phototropin blue-light receptors. *Annu Rev Plant Biol* **58**, 21-45

[45] Briggs WR (2007) The LOV domain: a chromophore module servicing multiple photoreceptors. *J Biomed Sci* **14**, 499-504

[46] Swartz TE, Corchnoy SB, Christie JM, Lewis JW, Szundi I, Briggs WR, Bogomolni RA (2001) The photocycle of a flavin-binding domain of the blue light photoreceptor phototropin. *J Biol Chem* **276**, 36493-36500

[47] Salomon M, Christie JM, Knieb E, Lempert U, Briggs WR (2000) Photochemical and mutational analysis of the FMN-binding domains of the plant blue light receptor, phototropin. *Biochemistry* **31**, 9401-9410

[48] Salomon M, Eisenreich W, Durr H, Schleicher E, Knieb E, Massey V, Rudiger W, Müller F, Bacher A, Richter G (2001) An optomechanical transducer in the blue light receptor phototropin from Avena sativa. *Proc Natl Acad Sci USA* **98**, 12357-12361

[49] Crosson S, Moffat K (2001) Structure of a flavin-binding plant photoreceptor domain: Insights into light-mediated signal transduction. *Proc Natl Acad Sci USA* **98**, 2995-3000

[50] Crosson S, Moffat K (2002) Photoexcited structure of a plant photoreceptor domain reveals a light-driven molecular switch. *Plant Cell* **14**, 1067-1075

[51] Fedorov R, Schlichting I, Hartmann E, Domratcheva T, Fuhrmann M, Hegemann P (2003) Crystal structures and molecular mechanism of a light-induced signaling switch: The Phot-LOV1 domain from Chlamydomonas reinhardtii. *Biophys J* **84**, 2474-2482

[52] Kasahara M, Swartz TE, Olney MA, Onodera A, Mochizuki N, Fukuzawa H, Asamizu E, Tabata S, Kanegae H, Takano M, Christie JM, Nagatani A, Briggs WR (2002) Photochemical properties of the flavin mononucleotide-binding domains of the phototropins from Arabidopsis, rice, and Chlamydomonas reinhardtii. *Plant Physiol* **129**, 762-773

[53] Swartz TE, Tseng TS, Frederickson MA, Paris G, Comerci DJ, Rajashekara G, Kim JG, Mudgett MB, Splitter GA, Ugalde RA, Goldbaum FA, Briggs WR, Bogomolni RA (2007) Blue-light-activated histidine kinases: Two-component sensors in bacteria. *Science* **317**, 1090-1093

[54] Kasahara M, Swartz TE, Olney MA, Onodera A, Mochizuki N, Fukuzawa H, Asamizu E, Tabata S, Kanegae H, Takano M, Christie JM, Nagatani A, Briggs WR (2002) Photochemical Properties of the Flavin Mononucleotide-Binding Domains of the Phototropins from Arabidopsis, Rice, and Chlamydomonas reinhardtii. *Plant Physiol* **129**, 762-773

[55] Bittl R, Kay CWM, Weber S, Hegemann P (2003) Characterization of a Flavin Radical Product in a C57M Mutand of a LOV1 Domain by Electron Paramagnetic Resonance. *Biochemistry* **42**, 8506-8512

[56] Martínez JI, Alonso PJ, Gómez-Moreno C, Medina M (1997) One- and Two-Dimensional ESEEM Spectroscopy of Flavoproteins. *Biochemistry* **36**, 15526-15537

[57] Medina M, Lostato A, Sancho J, Gómez.Moreno C, Cammack R, Alonso P, Martínez JI (1999) Electron-Nuclear Double Resonance and Hyperfine Sublevel Correlation Spectroscopic Studies of Flavodoxin Mutants from Anabaena sp. PCC 7119. *Biophys J* **77**, 1712-1720

[58] Weber S, Richter G, Schleicher E, Bacher A, Mobius K, Kay CWM (2001) Substrate binding to DNA photolyase studied by electron paramagnetic resonance spectroscopy. *Biophys J* **81**, 1195-1204

[59] Eriksson LE, Ehrenberg A, Hyde JS (1970) Comparative electron-nuclear double resonance study of two flavoproteins. *FEBS* **17**, 539-543

[60] Hyde JS, Rist GH, Eriksson LE (1968) Endor of methyl matrix and alpha protons in amorphous and polycristalline matrices. *J Phys Chem* **72**, 4269

[61] Mees A, Klar T, Gnau P, Hennecke U, Eker APM, Carell T, Essen LO (2004) Crystal structure of a photolyase bound to a CPD-like DNA lesion after in situ repair. *Science* **306**, 1789-1793

[62] Stehlik D, Möbius K (1997) New EPR methods for investigating photoprocesses with paramagnetic intermediates. *Annu Rev Phys Chem* **48**, 745-784

[63] Bittl R, Weber S (2005) Transient radical pairs studied by time-resolved EPR. *Biochim Biophys Acta* **1707**, 117-126

[64] Furrer R, Thurnauer MC (1981) Nanosecond time resolution in electron-electron.paramagnetic-res transient nutation spectroscopy of triplet-states. *Chem Phys Lett* **79**, 28-33

[65] van Tol J, Brunel LC, Angerhofer A (2001) Transient EPR at 240 GHz of the excited triplet state of free-base tetra-phenyl porphyrin. *Appl Magn Res* **21**, 335-340

[66] van Tol J, Brunel LC, Wylde RJ (2005) A quasioptical transient electron spin resonance spectrometer operating at 120 and 240 GHz. *Rev Sci Instrum* **76**, 074101

[67] Lin CT, Todo T (2005) The cryptochromes.*Genome Biol* **6**, 220

[68] Weber S, Kay CWM, Mogling H, Mobius K, Hitomi K, Todo T (2002) Photoactivation of the flavin cofactor in Xenopus laevis (6-4) photolyase: Observation of a transient tyrosyl radical by time-resolved electron paramagnetic resonance. *Proc Natl Acad Sci USA* **99**, 1319-1322

[69] Biskup T, Schleicher E, Okafuji A, Link G, Hitomi K, Getzoff ED,,Weber S (2009) Direct Observation of a Photoinduced Radical Pair in a Cryptochrome Blue-Light Photoreceptor. *Angew Chem Int Ed* **48**, 404-407

[70] Cashmore AR (2003) Cryptochromes: Enabling plants and animals to determine circadian time. *Cell* 114, 537-543

[71] Brudler R; Hitomi K; Daiyasu H; Toh H; Kucho K; Ishiura M; Kanehisa, M; Roberts VA; Todo T; Tainer JA; Getzoff ED (2003) Identification of a new cryptochrome class: Structure, function, and evolution. *Molecular Cell* 11, 59-67

[72] Devlin PF; Kay SA (2001) Circadian photoperception. *Ann. Rev. Phys.* 63, 677-694

[73] Canamero RC; Bakrim N; Bouly JP; Garay A; Dudkin EE; Habricot Y; Ahmad M (2006) Cryptochrome photoreceptors cry1 and cry2 antagonistically regulate primary root elongation in Arabidopsis thaliana. *Plant A* 224, 995-1003

[74] Ahmad M; Jarillo JA; Smirnova O; Cashmore AR (1998) Cryptochrome blue-light photoreceptors of Arabidopsis implicated in phototropism. *Nature* 392, 720-723

[75] Li YF, Heelis PF; Sancar A (1991) Active-site of DNA photolyase – Tryptophan-306 is the intrinsic jydrogen-atom donor essential for flavin radical photoreduction and DNA-repair in vitro. *Biochemistry* **30**, 6322-6329

[76] Lukacs A, Eker APM, Byrdin M, Brettel K, Vos MH (2008) Electron Hopping through the 15 angstrom Triple Tryptophan Molecular Wire in DNA Photolyase Occurs within 30 ps. *J Am Chem Soc* **130**, 14394

[77] Byrdin M, Sartor V, Eker APM, Vos MH, Aubert C, Brettel K, Mathis P (2004) Intraprotein electron transfer and proton dynamics during photoactivation of DNA photolyase from E-coli: review and new insights from an "inverse" deuterium isotope effect. *Biochim Biophys Acta* **1655**, 64-70

[78] Zeugner A, Byrdin M, Bouly JP, Bakrim N, Giovani B, Brettel K, Ahmad M (2005) Light-induced electron transfer in Arabidopsis cryptochrome-1 correlates with in vivo function. *J Biol Chem* **280**, 19437-19440

[79] Milov AD, Salikhov KM, Shirov MD (1981) Application of ENDOR in electron-spin echo for paramagnetic center space distribution in solids. *Fizika Tverdogo Tela* **23,** 975-982

[80] Jeschke G (2002) Distance Measurements in the Nanometer Range by Pulse EPR. *ChemPhysChem* **3**, 927–932

[81] Martin RE, Pannier M, Diederich F (1998) Determination of end-to-end distances in a series of TEMPO diradicals of up to 2.8 nm length with a new four-pulse double electron electron resonance experiment. *Angew Chem Int Ed* **37**, 2834-2837

[82] Millhauser GL (1992) Selective placement of electron-spin-resonance spin labels – New structural methods for peptides and proteins. *Trends Biochem Sci* **17**, 448-452

[83] Hubbell WL, Altenbach C, Hubbell CM, Khorana HG (2003) Rhodopsin structure, dynamics, and activation: A perspective from crystallography, site-directed spin labeling, sulfhydryl reactivity, and disulfide cross-linking. *Adv Protein Chem* **63**, 243-290

[84] Jeschke G, Panek G, Godt A, Bender A, Paulsen H (2004) Data Analysis Procedures for Pulse ELDOR Measurements of Broad Distance Distributions. *Appl Magn Reson* **26**, 223-244

[85] Swanson MA, Kathirvelu V, Majtan T, Frerman FE, Eaton GR, Eaton SS (2009) DEER Distance Measurement Between a Spin Label and a Native FAD Semiquinone in Electron Transfer Flavoprotein. *J Am Chem Soc* **131**, 15978-15979

[86] Kay CWM, Elsässer C, Bittl R, Farrell SR, Thorpe C (2006) Determination of the distance between the two neutral flavin radicals in augmenter of liver regeneration by pulsed ELDOR. *J Am Chem Soc* **128**, 76-77

[87] Daiyasu H, Ishikawa T, Kuma K, Iwai S, Todo T, Toh H (2004) Identification of cryptochrome DASH from vertebrates. *Genes Cells* **9**, 479-495

Figures

Figure 1: Continuous wave EPR spectra at 360GHz and high magnetic field. Left: Anionic FAD radical of *Aspergillus niger* glucose oxidase at pH 10, 140K. Right: Neutral FAD radical of *Escherichia coli* CPD photolyase, 200K. The respective flavin structure diagrams are shown below. Adapted from [20, 30].

Figure 2: Structure of the neutral flavin radical. Red arrows indicate positions which are positively identifiable by ENDOR spectroscopy, shaded red for protons with weaker couplings, which will show up in the matrix region of the ENDOR spectrum (< 2MHz coupling). The positions indicated by blue arrows can unequivocally be identified by 2D-ESEEM spectroscopy [20, 56]**.**

Figure 3: X-band ENDOR spectra of *Aspergillus niger* glucose oxidase in two pH conditions recorded at 80K. Top: At pH 10, the protein forms an anionic radical which exhibits a large H(8α) coupling and lacks the H(5) signal. Bottom: At more acidic conditions, there is a neutral flavin radical instead. H(5) is clearly visible. Adapted from [20].

Figure 4: Top: Cutout from the crystal structure of *Xenopus laevis* (6-4) photolyase (pdb entry: '1TEZ'), highlighting the active histidines in their protonation state as well as the flavin cofactor. Bottom: X-Band ENDOR spectra of this protein's wild type with His354Ala and His358Ala mutations below. Red H(8α) and blue H(1') curves show these proton's contributions to the overall signal. Adapted from [61, 22].

Figure 5: X-band ENDOR spectra of the neutral flavin radical in C(4a)-inhibited *Avena sativa* phototropin 1 LOV2 domain C450A. Below, several additional mutations in the vicinity of H8α. Left: Spectra recorded at 120 K (dashed lines), 80 K (black lines) and 10 K (shaded gray). Right: Detail of the 10 K-spectra (dotted line) with simulations of the spectral contributions of both H(1') protons (green), H(6) (blue) and H(8α) (red), including a residual isotropic coupling (orange) where necessary. Superpositions of all simulated tensors are shown in solid black. Adapted from [21].

Figure 6: Left: DFT calculations of H(8α) hyperfine couplings as a function of the rotation angle of the 8α methyl group (gray lines). The dots mark the isotropic hyperfine couplings of both methyl protons possible to obtain from the measurements (see figure 5). Set in is a schematic side view of the isoalloxazine plane and the determined rotation angles in case of Cys450Ala and Cys450Ala/Asn425Cys. Right, top: Temperature behavior of the isotropic H(8α) coupling peak amplitude for all examined mutations of *A. sativa* LOV2 as well as for inhibited *C. reinhardtii* phototropin LOV2 Cys250Ser. Right, bottom: Direct comparison of X-band ENDOR spectra of *A. sativa* LOV2 Cys450Ala/Asn425Cys and *C. reinhardtii* LOV2 Cys250Ser at 80K and 10K. Adapted from [21].

Figure 7: X-band cw-ENDOR spectra of pure *E. coli* CPD photolyase (dotted line) and bound to CPD substrate (solid black), recorded at 160K. All panels show the designated coupling frequency

regions of all strongly coupled protons, the arrows indicate the corresponding RF frequency axes. Adapted from [58].

Figure 8: Transient EPR spectra at X-band (left) and Q-band frequencies (right) of *Synechocystis* cryptochrome-DASH at 274K and 272K, respectively. Below, simulations of radical pair spectra for a polarized triplet, a thermalized triplet and a singulet precursor are shown. Adapted from [10].

Figure 9: Top: Transient X-band EPR spectrum of *X. laevis* cryptochrome-DASH [87] (blue) with simulation (dashed blue) and of the W324F mutant (green), in which the distal tryptophan was replaced, both at 274K. Below, cutout from a model structure of *X. laevis* cryptochrome-DASH (sequence code: 'Q75WS4'), illustrating the electron transfer chain from the flavin to the distal tryptophan. Bottom: Transient X-band EPR spectra of *Synechocystis* cryptochrome-DASH (blue) with simulation (dashed red) and of the W320F, W373F and W375F mutants (green), 274K. Below, cutout from the crystal structure of *Synechocystis* sp. cryptochrome-DASH (pdb entry: '1NP7') [71], showing the alternative terminal tryptophan W375 in the electron transfer chain. Adapted from [12, 69, 71].

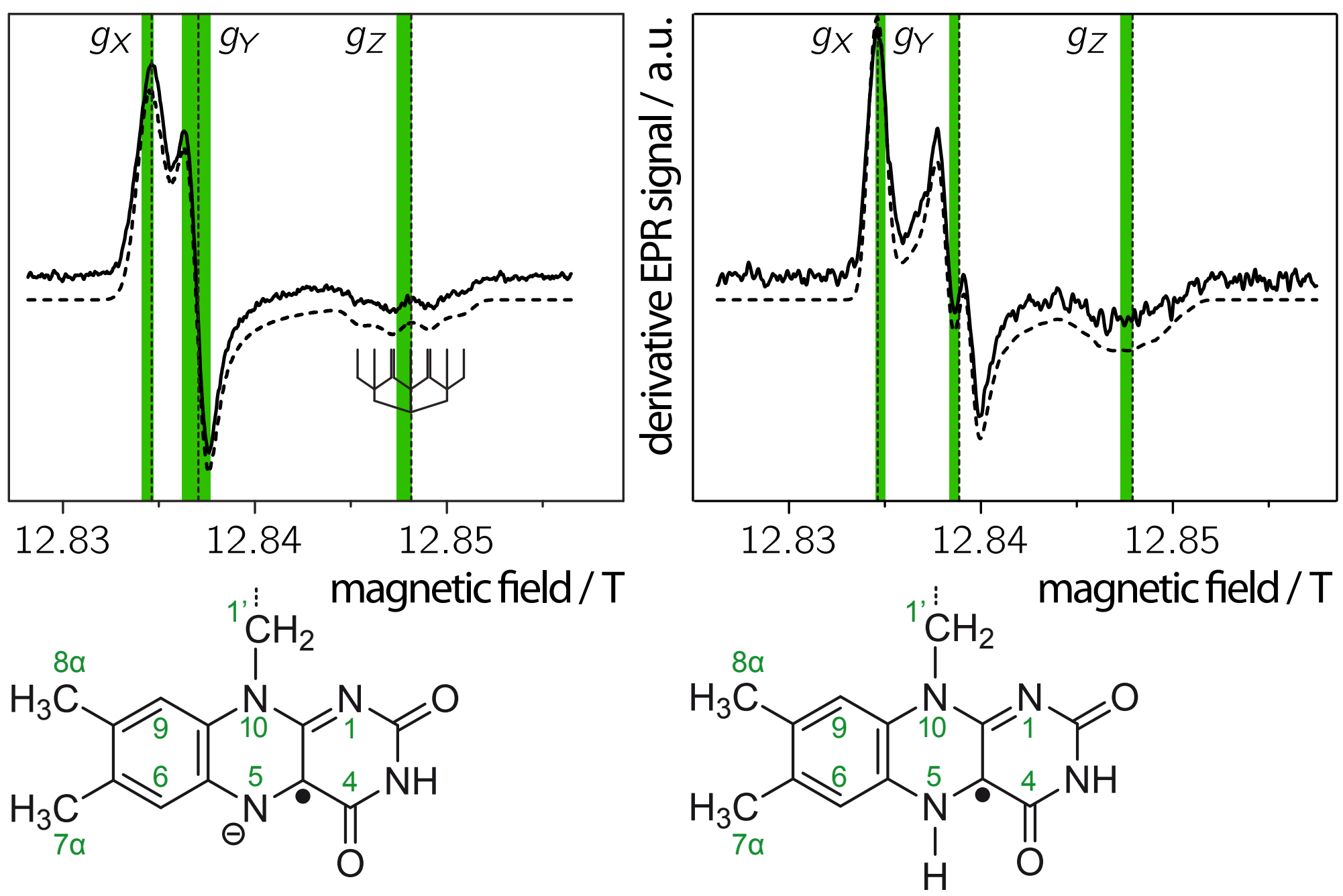
gX
gY
gZ
12.83
12.84
12.85
magnetic field / T
derivative EPR signal / a.u.
gX
gY
gZ
12.83
12.84
12.85
magnetic field / T
1'
CH2
8α
H3C
N
N
O
9
10
1
6
5
4
NH
H3C
7α
N
O
1'
CH2
8α
H3C
N
N
O
9
10
1
6
5
4
NH
H3C
7α
N
H
O

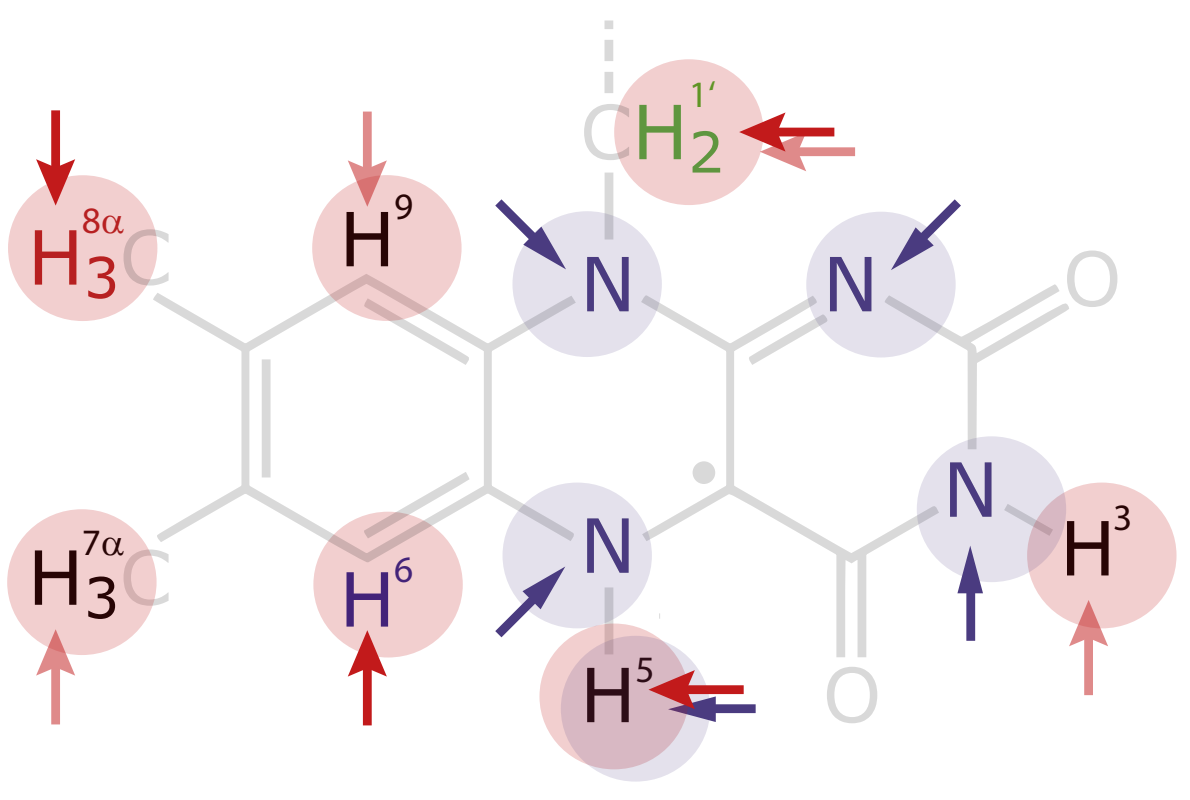
H3 8α
H 9
H2 1′
N
N
O
N
H 3
H3 7α
H 6
N
H 5
O

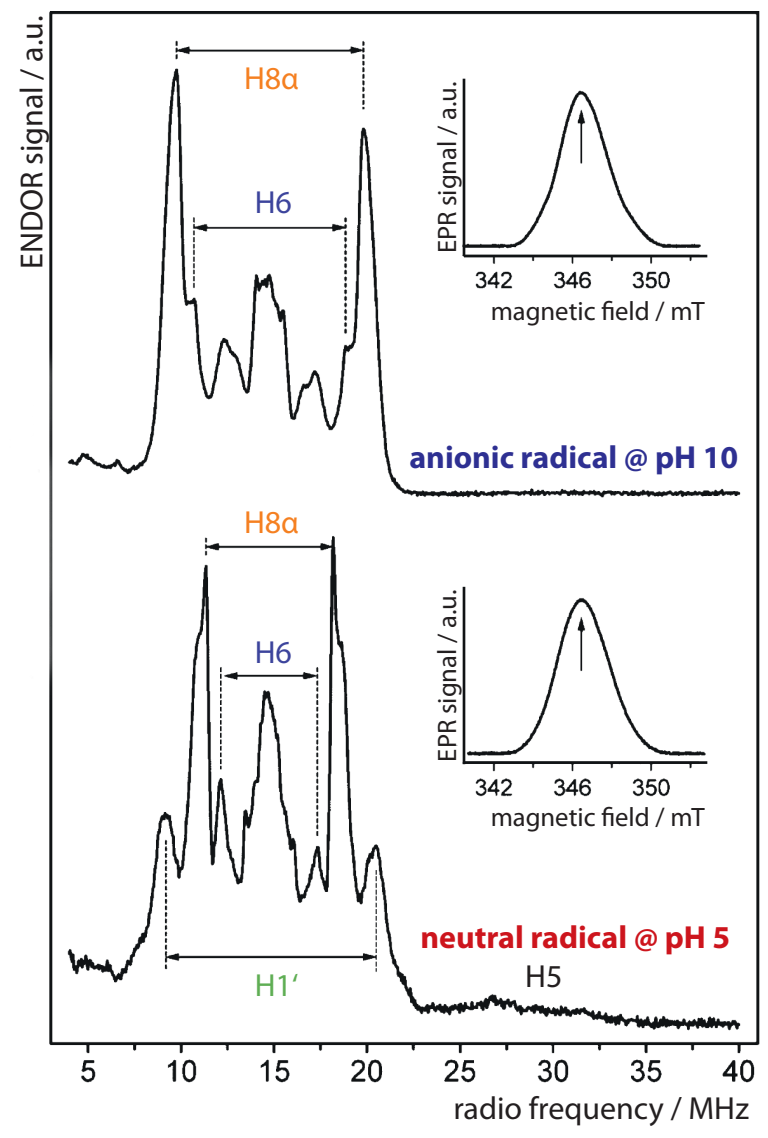
ENDOR signal / a.u.
H8α
H6
EPR signal / a.u.
342
346
350
magnetic field / mT
anionic radical @ pH 10
H8α
H6
EPR signal / a.u.
342
346
350
magnetic field / mT
neutral radical @ pH 5
H5
H1′
5
10
15
20
25
30
35
40
radio frequency / MHz

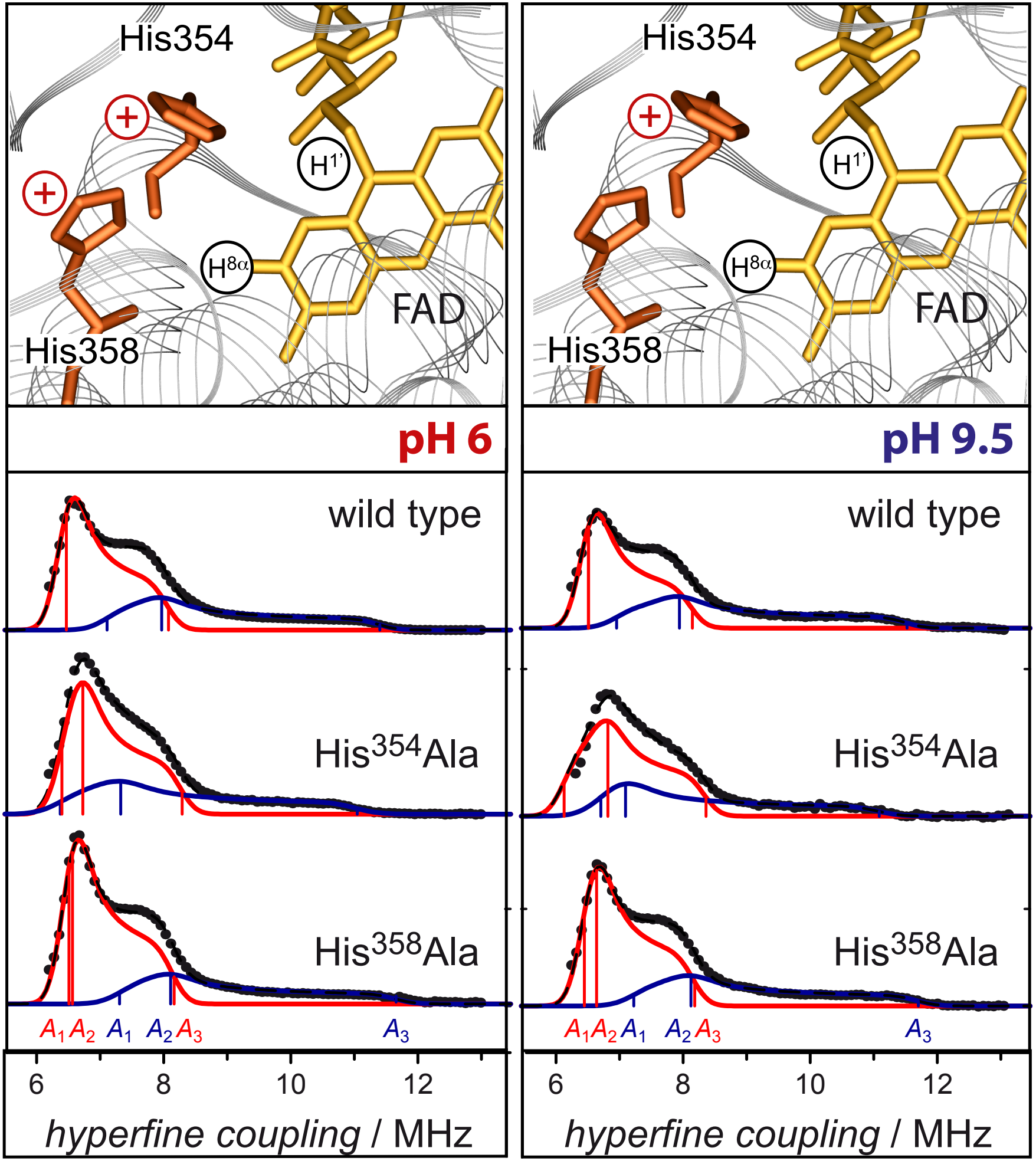
His354
H1'
H8α
FAD
His358
pH 6
pH 9.5
wild type
His354Ala
His358Ala
A1 A2 A1 A2 A3
A3
6
8
10
12
hyperfine coupling / MHz

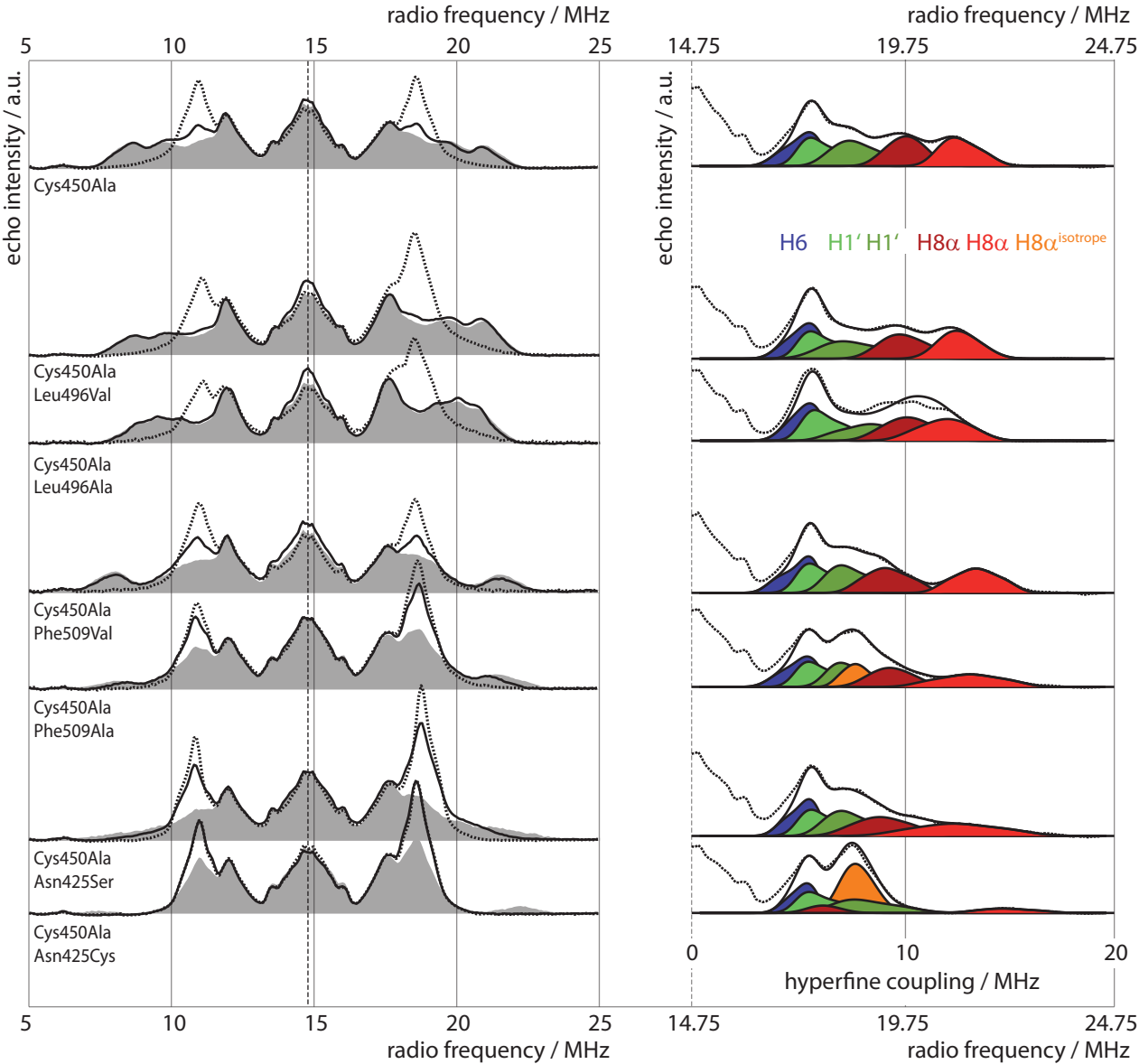
radio frequency / MHz
5
10
15
20
25
14.75
19.75
24.75
echo intensity / a.u.
Cys450Ala
Cys450Ala
Leu496Val
Cys450Ala
Leu496Ala
Cys450Ala
Phe509Val
Cys450Ala
Phe509Ala
Cys450Ala
Asn425Ser
Cys450Ala
Asn425Cys
H6
H1' H1'
H8α H8α
H8α isotrope
0
10
20
hyperfine coupling / MHz

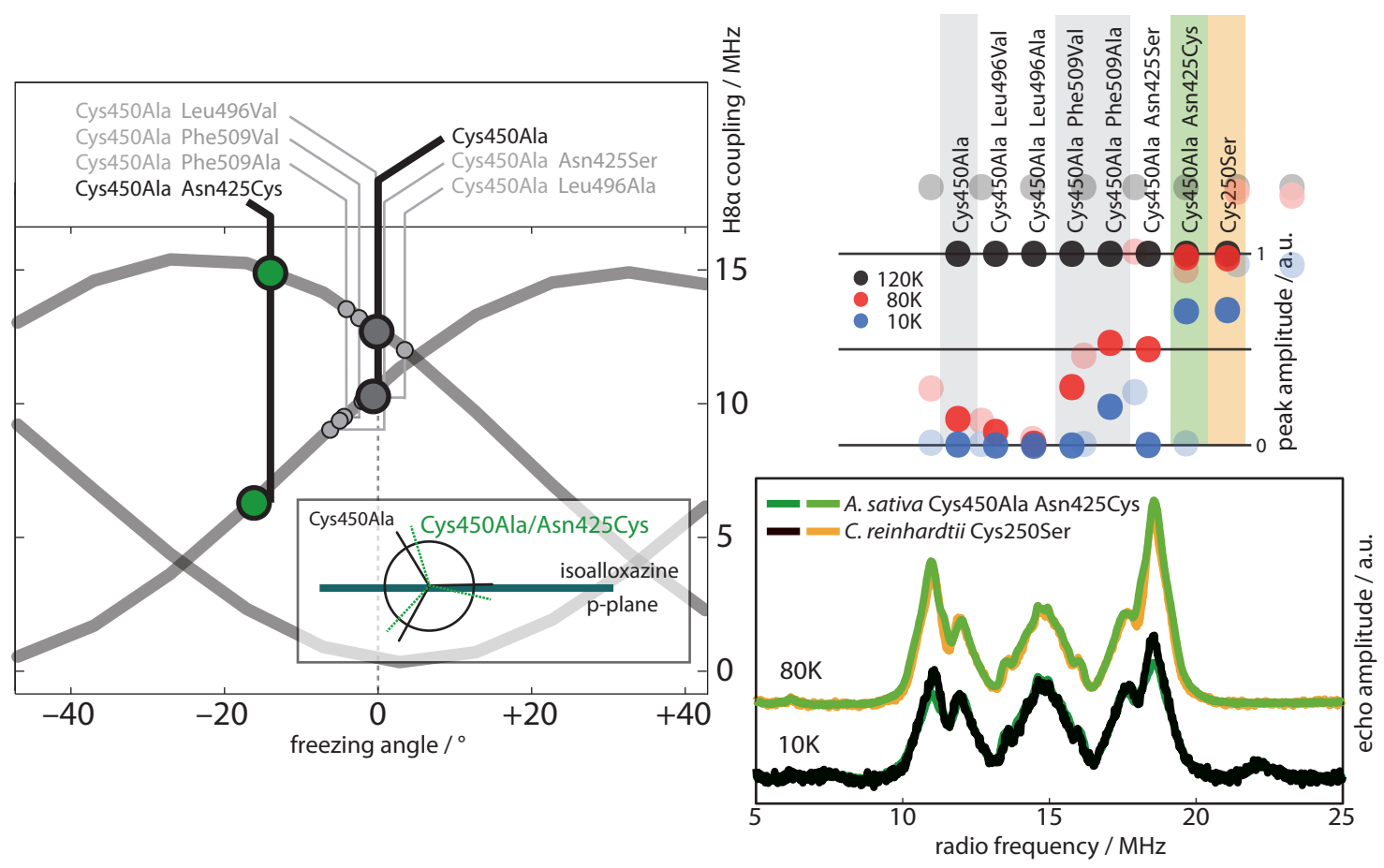
Cys450Ala Leu496Val
Cys450Ala Phe509Val
Cys450Ala Phe509Ala
Cys450Ala Asn425Cys
Cys450Ala
Cys450Ala Asn425Ser
Cys450Ala Leu496Ala
Cys450Ala
Cys450Ala/Asn425Cys
isoalloxazine
p-plane
H8α coupling / MHz
15
10
5
0
−40
−20
0
+20
+40
freezing angle / °
Cys450Ala
Cys450Ala Leu496Val
Cys450Ala Leu496Ala
Cys450Ala Phe509Val
Cys450Ala Phe509Ala
Cys450Ala Asn425Ser
Cys450Ala Asn425Cys
Cys250Ser
120K
80K
10K
1
0
peak amplitude / a.u.
A. sativa Cys450Ala Asn425Cys
C. reinhardtii Cys250Ser
80K
10K
5
10
15
20
25
radio frequency / MHz
echo amplitude / a.u.

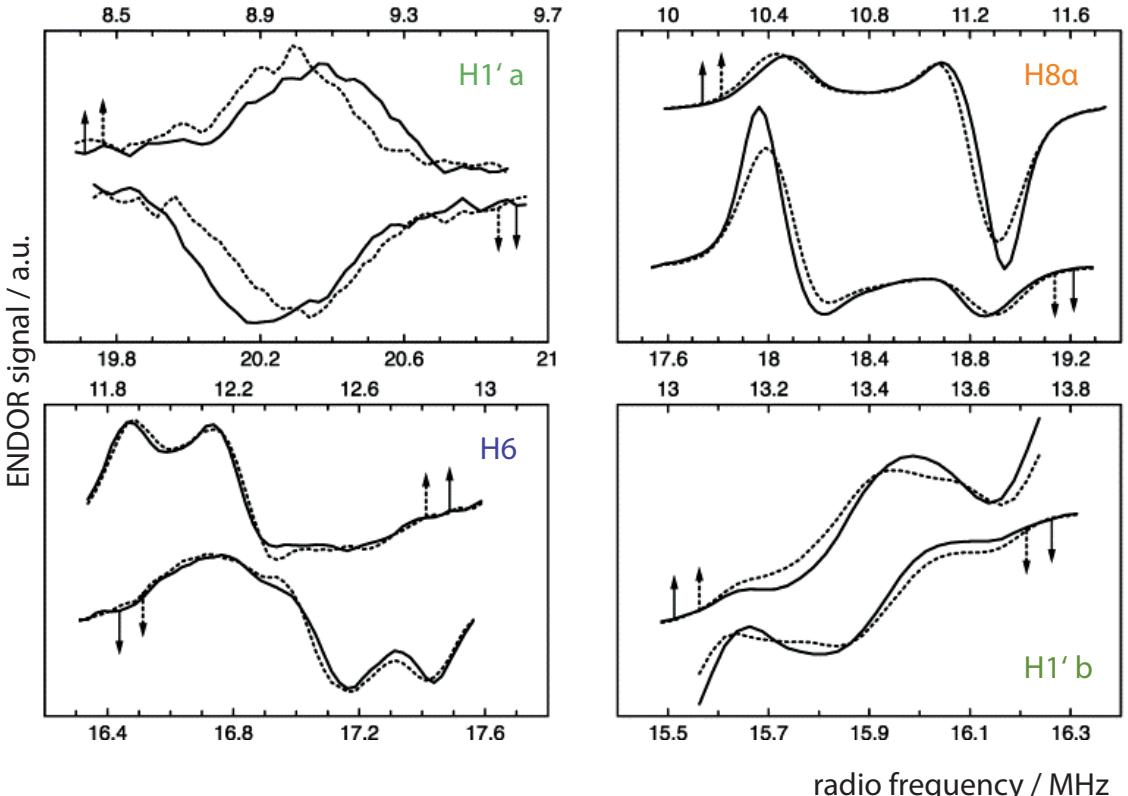
8.5
8.9
9.3
9.7
H1′ a
19.8
20.2
20.6
21
10
10.4
10.8
11.2
11.6
H8α
17.6
18
18.4
18.8
19.2
11.8
12.2
12.6
13
H6
16.4
16.8
17.2
17.6
13
13.2
13.4
13.6
13.8
H1′ b
15.5
15.7
15.9
16.1
16.3
ENDOR signal / a.u.
radio frequency / MHz

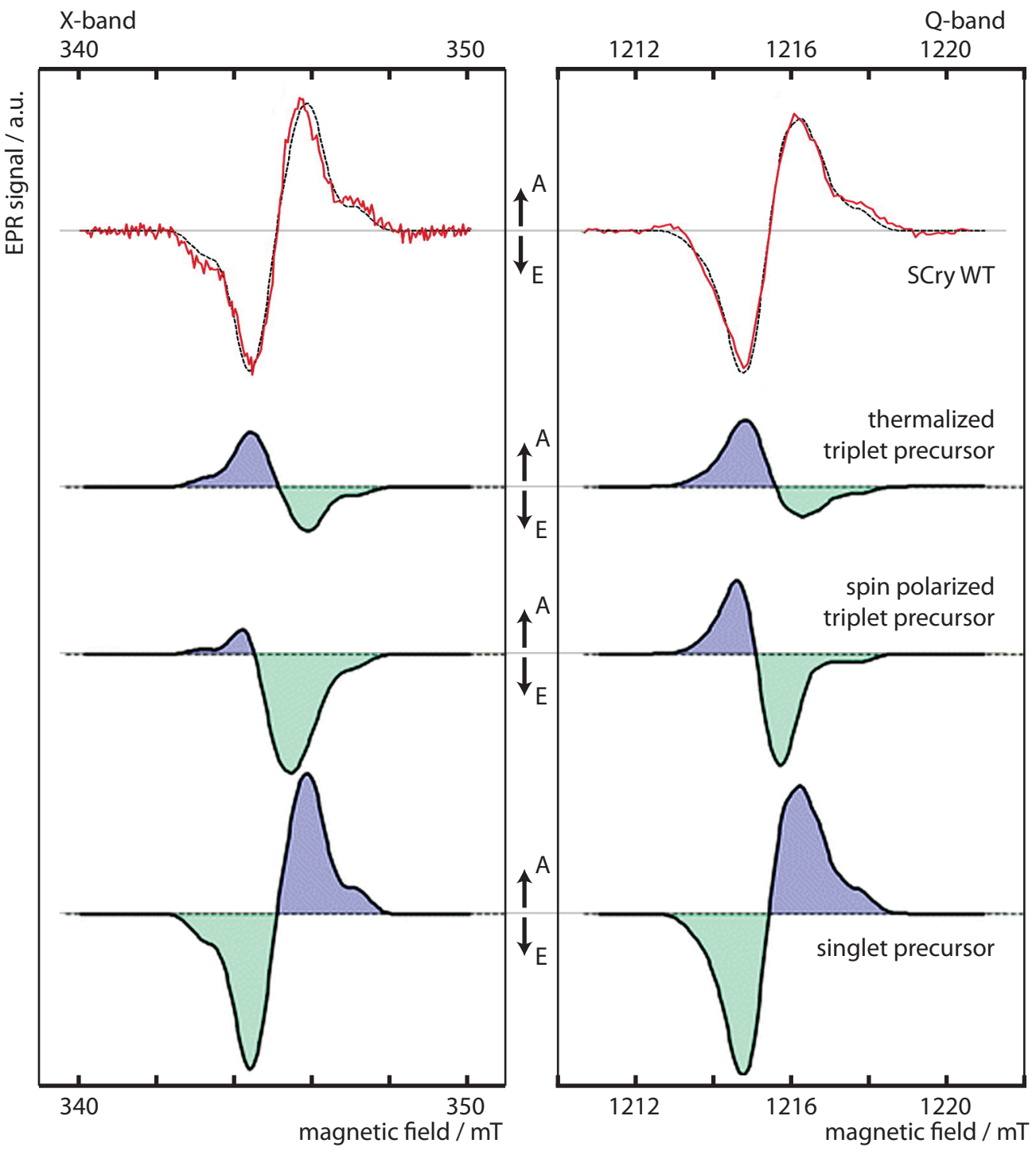
X-band
340
350
Q-band
1212
1216
1220
EPR signal / a.u.
A
E
SCry WT
thermalized
triplet precursor
spin polarized
triplet precursor
singlet precursor
340
350
magnetic field / mT
1212
1216
1220
magnetic field / mT

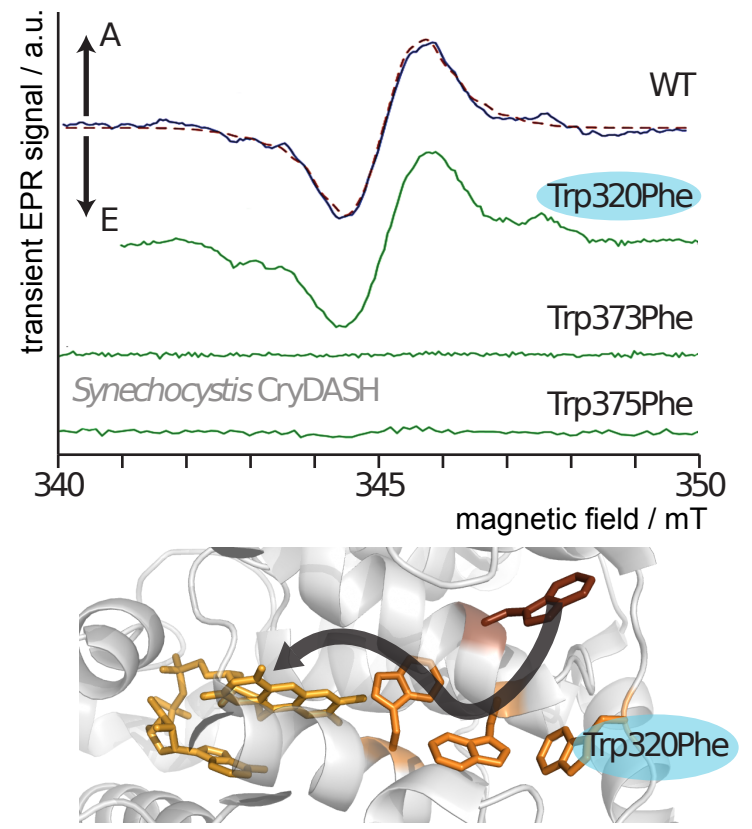
transient EPR signal / a.u.
A
E
WT
Trp320Phe
Trp373Phe
Synechocystis CryDASH
Trp375Phe
340
345
350
magnetic field / mT

Trp320Phe

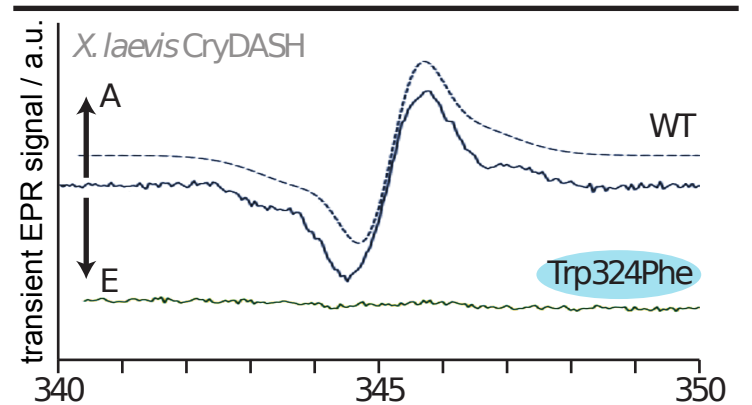
X. laevis CryDASH
transient EPR signal / a.u.
A
E
WT
Trp324Phe
340
345
350
magnetic field / mT